HIWPP non-hydrostatic dynamical core tests: Results from 3-km, three-day simulations

Jeffrey Whitaker and Philip Pegion
NOAA/ESRL/PSD
(per email: uploaded 20150604)

Background:

NCEP's current operational global atmospheric model dynamical core, the GSM, or Global Spectral Model, has been evolving but in continuous use for over 30 years. The horizontal resolution of the GSM (~13-km in 2015) is approaching a grid spacing at which cloud processes can no longer be treated through parameterizations; explicit predictions with non-hydrostatic assumptions will be required. In addition, the current GSM may not be able to scale up to take advantage of peta- and exascale high-performance computing (HPC) systems. These factors will require adoption of a new atmospheric dynamical core (dycore) for operational global prediction in the NWS within a decade. Since the global model touches almost every operational forecast NCEP produces, transitioning a new dycore into operations is difficult and costly. Therefore, the NWS needs to ensure the new dynamical core is "future proof" and can serve NOAA's needs for at least 20 years. The HIWPP (Sandy-Supplemental funded High Impact Weather Prediction Project) and NGGPS (Next-Generation Global Prediction System) projects are collaborating to evaluate candidate non-hydrostatic dynamical cores with a battery of tests. The initial phase included a series of idealized tests, inspired by the Dynamical Core Model Inter-comparison Project of 2012 (DCMIP; https://earthsystemcog.org/projects/dcmip-2012), a series of performance and scalability benchmarks, and two real-data forecast tests at ~ 3-km global grid spacing. The results of the real-data ~ 3-km forecast tests are summarized in this report. The results of the idealized tests and the performance benchmarks are summarized in separate reports.

Participating Dynamical Cores:

The five candidate dycores are listed below, with sponsors in parentheses and descriptions of physics packages used.

- **FV3** (GFDL) – Cubed sphere grid, finite-volume discretization (a non-hydrostatic version of the hydrostatic core described in Lin (2004). The physics packages were from the GFDL AM4 and AM3 climate models, as described in Donner (2011), except where noted below:
    - A newly developed GFDL double-plume convective parameterization was used. The entrainment rates were increased so that plumes detrain quickly, allowing explicit simulation of moist convection to dominate.
    - The stable PBL parameterization was turned off.
    - Six-category cloud micro-physics was included, as described by Chen and Lin (2013)
    - The PBL scheme is the same as GFDL AM3.

    - Rivers and lakes were not included in the land-surface model, and other input land surface datasets were interpolated from a 50-km resolution dataset.
- **MPAS** (NCAR) – Unstructured icosahedral grid with C-grid variable staggering (Skamarock et al. 2012). Physics packages used:
    - RRTMG long and short-wave radiation.
    - No deep convective parameterization.
    - WSM6 microphysics.
    - Mellor-Yamada surface layer scheme.
    - YSU PBL scheme.
- **NEPTUNE** (NRL) – Flexible cubed sphere or icosahedral grid using a spectral element discretization with the Non-hydrostatic Unified Model of the Atmosphere (NUMA) core (Giraldo et al. 2014). Did not submit results for this test.
- **NIM** (ESRL) – Non-hydrostatic Icosahedral Model (unstaggered finite-volume, A-grid implementation). Operational GFS physics used, including deep convective parameterization.
- **NMMUJ** (EMC) – Finite-difference, cubed-sphere grid version of the B-grid lat/lon grid dycore described in Janjic and Gall (2012). The construction of the 'uniform Jacobian' cubed sphere grid is described in NCEP Office Note 467, available at http://www.lib.ncep.noaa.gov/ncepofficenotes/2010s/.
  Physics packages used (from operational NAM):
    - RRTMG long and short-wave radiation.
    - Betts-Miller-Janjic deep convective parameterization.
    - Ferrier microphysics.
    - Mellor-Yamada-Janjic surface layer and turbulence scheme.

Experimental Design:

The goal was to 'stress-test' the dynamical cores by running them at global cloud-permitting resolution, with full physics, initial conditions derived from an operational data assimilation system, and high-resolution orography. Two sets of initial conditions were provided to the modeling groups (18 UTC October 24, 2012, and 00 UTC 18 May 2013), both produced by the operational NCEP T1534 hybrid 3D ensemble-variational data assimilation system. Forecasts were run to +72 hours, with selected fields output at hourly resolution.

The October 2012 case was chosen to illustrate the ability of the dynamical cores to represent the fine-scale structures in the inner core of tropical cyclones. The period October 25-27, 2012 covers the initial stages of development of Hurricane Sandy, as it crossed the complex terrain of Cuba, weakened and then re-intensified near the Bahamas. At the same time, Typhoon Son-Tinh intensified west of the Philippines, making landfall in Southern China on October 28.

The May 18-20 period covers several consecutive days of severe weather over the U.S. Great Plains, including a violent tornado that devastated the town of Moore, OK on May

20. This case was chosen to illustrate the ability of the models to represent the structure of supercell thunderstorms that often spawn tornados.

Each modeling group used its own physical parameterization suite. Further tests are planned with a standard physics package (from the operational GFS model) implemented in each model. Since all of the models are in an early stage of development, none of them have well-tuned physics. As a result, we will not emphasize the skill of the model forecasts. Issues in the forecasts likely related to physics will be noted, but *the main focus of this evaluation will be on the ability of the models to realistically represent features that are not currently well resolved in today's operational models and that will require non-hydrostatic dynamics to represent accurately*. Characteristics of globally integrated quantities (such as dry mass, total precipitation, and integrated water vapor) are presented, as well as kinetic-energy and vertical-velocity spectra.

Globally integrated diagnostics

Figure 1 shows the 72-h forecast global kinetic-energy spectra at 200 hPa for the October 2012 case, as a function of total wavenumber, ranging from wavenumber 10 to wavenumber 7200. The spectra were computed using spherical harmonic transforms of the 0.025 degree lat/lon data provided by the modeling groups. The spectra for the current operational T1534 GFS, and the operational ECMWF model forecast from 2012, are also shown. Two reference lines are plotted on the figure, one showing the slope of a -3 power-law spectrum (consistent with two-dimension turbulence theory and synoptic-scale motions) and one showing the slope of a -5/3 power-law spectrum (consistent with fully three-dimensional turbulence and mesoscale motions). Vertical lines indicate wavelengths corresponding to twice the grid resolution (6 km), four times the grid resolution (12 km), and eight times the grid resolution (24 km). All of the models show a steeper slope at wavelengths greater than 500 km, similar to the -3 slope predicted by two-dimensional turbulence theory (and captured by current operational hydrostatic forecast models). The MPAS, NMMUJ and FV3 spectra transition to a shallower slope at wavelengths less than a few hundred kilometers, which agrees qualitatively with what would be expected from three-dimensional turbulence theory. The NIM kinetic-energy spectrum does not exhibit a mesoscale transition and falls off rapidly starting at wavelengths around 100 km, indicating the model is heavily damped. MPAS appears to have less energy at intermediate scales (1000-100km), but the reason for this is not clear. The scale of the numerical diffusion in NMMUJ, FV3 and MPAS is evident at the tail end of the spectra, at around six to eight times the grid spacing (around 20-km), where the slope steepens. NIM has almost four orders of magnitude less energy at the 20-km scale than the other models. The orography used in the NIM forecasts is also very smooth (Figure 2). From the orography spectra (Figure 3), it appears that FV3 used a somewhat larger filter scale for the orography than MPAS or NMMUJ, and the NIM orography was very heavily filtered.

The main conclusion of the kinetic energy spectra evaluation is that while FV3, MPAS and NMMUJ all show the expected transition to a shallower spectral slope in the mesoscale, NIM appears to be highly damped without significant variability at scales less

than 50-100 km. For unknown reasons, MPAS appears to have less energy in intermediate scales (100-1000 km) than the other models. The orography used in the forecasts was very smooth in NIM, while FV3 used somewhat more heavily filtered orography than MPAS or NMMUJ.

Vertical velocity spectra at 500 hPa for the May 2013 case are shown in Figure 4. Ecklund et al. (1986) suggest, based on radar observations and the theory of internal gravity waves, that in quiet conditions vertical velocity spectra should be basically white (flat), down to wavelengths associated with the Brunt-Väisälä frequency. Under windy conditions, their results suggests that the spectra should be steeper, close to the -5/3 spectra slope seen with horizontal winds. This is because the isentropic surfaces in frontal zones can become highly distorted, leading to isentropic motions with a significant vertical component. The radars used in that study observed clear air, and hence did not consider vertical motions associated with moist convection. Figure 4 shows that both MPAS and FV3 have vertical velocity spectra that are relatively flat (as compared to the kinetic-energy spectra), with peaks at synoptic scales (a few thousand km) and at six to eight times the grid resolution (20-30 km). The synoptic-scale peak is consistent with what would be expected from quasi-horizontal motions along sloping isentropic surfaces in mid-latitude baroclinic eddies. The high wavenumber peak is near the effective resolution of the models (usually around 6-8Δx) and is likely associated with grid-scale convection, gravity waves generated by convection and orography, and other marginally resolved, small-scale non-hydrostatic processes. The fact that the FV3 peak is at slightly larger scales than MPAS, with vertical velocity variance falling off more steeply at higher wavenumbers, indicates that convective processes are somewhat more damped in FV3 than MPAS. NMMUJ does not show a significant peak in vertical velocity variance at small scales. The reason for this is not clear. We hypothesize that it may be due to the effects of convective parameterization, and/or the presence of divergence damping in the dynamical core. MPAS does not have a deep convective parameterization. – FV3 does, but its effect is intentionally suppressed to allow resolved convection to dominate. NMMUJ has much less vertical velocity variance at all scales than MPAS and FV3 (and NIM at the largest scales), suggesting that the flow field is much more horizontal and convective motions significantly weaker at all scales. NIM lacks any variance in vertical velocity at scales less than a few hundred kilometers.

The main conclusions of the vertical velocity spectra evaluation are that

- FV3 and MPAS show a peak in vertical velocity variance at small scales, likely associated with the effects of marginally resolved convective processes.
- Diffusion limited the scale of FV3 convective updrafts more strongly than in MPAS.
- NIM lacks any variability at scales less than 50-100km.
- NMMUJ has weaker vertical velocities at large scales relative to NIM ,and at all scales relative to FV3 and MPAS, possibly due to the effects of divergence damping and/or convective parameterization

A more detailed analysis of the spectral obtained in 3-km MPAS forecasts is available in Skamarock et al (2014)

The conservation of globally integrated dry atmospheric mass during the forecasts was checked by looking at the evolution of the global mean dry surface pressure (not shown). MPAS, FV3 and NIM all appear to conserve total atmospheric dry mass. NMMUJ conserves total mass, but loses dry mass during the three day forecast period. Since the total mass of water vapor (Figure 5) increases during the integration, dry mass must decrease to compensate if the total mass is conserved.

The global-mean precipitation (Figure 6) spins up quickly to about 3 mm for all the models except NMMUJ, which continues to increase up to nearly 5.5 mm by day 3. The fact that both the total integrated water vapor and precipitation are increasing in NMMUJ suggests that there is excessive evaporation from the surface, but this could not be verified since evaporation was not archived.

A commonly used diagnostic of external mode gravity-wave noise is the global integral of surface pressure tendency variance. Figure 7 shows the global mean standard deviation of one hour surface pressure tendency during the 72-hour integration for the two cases. NIM clearly has dynamical imbalances that are exciting large amplitude external gravity waves. These are evident in maps of 1-hour surface pressure tendency (not shown), propagating at a speed close to the external gravity mode phase speed (roughly 300 meters per second). The amplitude of these waves decreases gradually during the forecast, but remains significant even at 72 hours. MPAS and FV3 have relatively low levels of external mode noise. The level of noise in the NMMUJ integration is somewhat larger, but still much less than in NIM.

The main conclusions regarding the evaluation of globally integrated quantities are that

- NMMUJ does not conserve dry mass.
- NMMUJ has an overactive hydrologic cycle, resulting in increasing precipitation and integrated water vapor during the forecasts.
- NIM has higher levels of external mode gravity wave noise during the integrations than the other models.

Hurricane Sandy Forecast Results

Forecasts were initialized from 18 UTC 24 October 2012, when Hurricane Sandy was located between Jamaica and Cuba. Analyses from the pre-implementation parallel runs of the T1534 GFS data assimilation system were provided to the modeling groups on the GFS native 3072x1536 grid (with 64 vertical levels). Each group performed their own interpolation to the higher-resolution model grids and substituted their own orographic and land-surface datasets. During the first 24 hours of the forecast, the storm crossed Cuba. None of the forecast models weakened the cyclone enough as the storm passed over the Cuba. NIM used an extremely smooth orography that did not resolve the high terrain over Cuba, while the FV3 terrain was somewhat smoother than MPAS and NMMUJ (Figure 8). Figure 9 shows the 10-m wind speeds for the 30-hour forecast valid

00UTC 26 October. Compared to the AOML/HRD radar wind analysis, all of the models except for NIM were slightly too strong at that time, and all of the models positioned the storm 50-100 km too far north. The NIM wind field is very smooth, with a much larger eye and radius of maximum wind than the other models. The 850-hPa relative vorticity fields illustrate the difference in effective resolution between NIM and the other models. MPAS and FV3 have a well-defined eye-wall ring of high vorticity with evidence of spiral rainbands. These features are absent in the NIM forecasts. The eye wall is also evident in the NMMUJ solution, however there is evidence of unphysical noise in the vorticity field at about 4-6 times the model grid resolution. This noise is particularly evident just north of the high terrain of Hispaniola. The vertical velocity field at 850 hPa (Figure 10) shows a similar level of detail in the FV3 and MPAS forecasts, and the same level of smoothness in the NIM solution. The FV3 vertical motion field appears to be somewhat smoother than MPAS. The NMMUJ vertical velocity field is much smoother than MPAS or FV3, but with significant noise near the grid scale. The vertical velocity in NMMUJ is also much smoother than its own vorticity field. This is consistent with the vertical velocity spectra shown in Figure 3. We hypothesize that this may be due to the influence of convective parameterization, and/or divergence damping in the dynamical core.

At the same time as Hurricane Sandy, Typhoon Son-Tinh was developing over the South China Sea. Figures 10 and 11 show the 850hPa vorticity and vertical velocity fields at 00UTC October 27 2012, 54 hours into the forecast. The same qualitative differences in 850hPa vorticity and vertical velocity structures between the model forecasts seen between the Hurricane Sandy case (Figures 10 and 11) are also evident in this case (Figures 12 and 13), including the extreme smoothness of the NIM solution, and the large-scale character of the NMMUJ vertical velocity field.

The general conclusions from the Hurricane Sandy case are that MPAS and FV3 simulate tropical cyclones with reasonable fine-scale detail broadly consistent with observations and our current understanding of tropical cyclone structure. NMMUJ also produces reasonable detail in the rotational wind field, albeit with some non-physical noise near the grid scale, but produces much weaker and smoother vertical circulations. NIM is extremely smooth and as configured does not provide the level of detail one would expect in a 3-km forecast.

Moore OK tornado forecast results

During May 18–20, 2013 there was a significant tornado outbreak that affected parts of Midwest and lower Great Plains. On May 18, 27 tornados were reported, mostly in Kansas and Nebraska. 34 tornados were reported in Kansas and Oklahoma on the May 19, including an EF4 near the town of Shawnee, OK. On May 20, a violent EF5 tornado struck Moore, OK and was one of 37 tornadoes reported stretching from north Texas into southern Illinois. Initial conditions from the T1534 GFS for 00 UTC 18 May 2013 were provided to the modeling groups, and 72-hour forecasts were run. Following is a selection of plots meant to illustrate the character of the convective-scale forecasts generated by each model. Forecast skill is not emphasized, since that will be highly

dependent of the physics packages which have not been well-tested or tuned in these models. Rather, we attempt to assess the ability of the dynamical core to represent the basic structure of the observed thunderstorms, given the limitations of the physics.

Figure 14 is a hyperlink to an animation of accumulated precipitation every hour during the 72-hour forecast period[1]. The HRRR 1-h forecast precipitation, as well as the NWS Stage-IV radar and gauge blended estimates are shown for reference. The HRRR and Stage-IV precipitation estimates show rainfall developing in thunderstorms along line over Oklahoma and eastern Kansas between 00 UTC and 03 UTC on the 19th, 20th and 21st. All of the models produce rainfall in this region on the first day, with MPAS producing the most rainfall and NMMUJ the least. The total cloud condensate animation (double click on Figure 15) shows that smooth nature of the NIM convection (consistent with the tropical cyclone results). NIM fails to capture the convection over Oklahoma that led to the development of the EF5 tornado in Moore, OK. MPAS and to a lesser extent FV3 and NMMUJ do produce convection in central and eastern OK between 00-05 UTC on the 20th. Figure 16 is a hyperlink to an animation of 2-m specific humidity and 10-m wind vectors. Outflow boundaries and associated cold (dry) pools are clearly evident in the MPAS and NMMUJ forecasts, particularly between 00 and 06 UTC on the 19th. These features are more difficult to detect in the FV3 and HRRR output and are absent in the NIM forecast. On the third day, MPAS and NMMUJ capture the development of a line of thunderstorms in eastern Oklahoma at the end of the forecast period (around 00 UTC 21 May). NIM does not produce convection in this region on the third day, and FV3 emphasizes convection further north and east in Missouri.

Zooming in on the convection in northwest Oklahoma for 27-h forecasts valid 03 UTC May 19 2013, Figures 17-19 show the detailed structure of the convective cells in the four models. The scale of the convective updrafts and downdrafts are somewhat larger in FV3 than in MPAS, consistent with the tropical cyclone plots (Figures 11 and 13) and the vertical velocity spectra (Figure 4). NIM produces unrealistically large scale updrafts. Outflow boundaries are clearly evident in the 850 hPa vertical velocity in both the FV3 and MPAS solutions. The character of the NMMUJ vertical velocity field is also broadly similar to the tropical cyclone case, in that there appears to be a larger scale pattern (perhaps associated with parameterized deep convection) superimposed on convective cells near the grid scale. Curiously, the vertical velocity at 850 hPa in the NMMUJ solution is highly anti-correlated with the vertical velocity at 500 hPa.

Overall, FV3, MPAS and NMMUJ all appear to capture some aspects of the severe convection observed over the south central Great Plains during this period with reasonable fine-scale detail. There are some puzzling aspects to the structure of the NMMUJ vertical velocity field, specifically the strong correspondence between sinking (rising) motion at 850 hPa and rising (sinking) motion at 500 hPa. The level of detail in

[1] The animation should open in your web browser when you double click on the figure, if you have an internet connection. If that does not work, cut and paste the URL in the figure caption into your web browser.

the convective forecast produced by NIM looks more like what would be expected from the current generation of global forecast models.

Summary

Four candidate non-hydrostatic dynamical cores were 'stress-tested' by running 3-km global forecasts with full physics and realistic orography for cases that included hurricanes and severe continental convection. The NIM solutions were unrealistically smooth and failed to capture the fine-scale detail one would expect in a 3-km forecast. This is consistent with the kinetic energy and vertical velocity spectra, which show very little variability at scales below 50-100 km in the NIM forecasts. FV3 and MPAS both produce realistic fine scale detail in tropical cyclones and regions of severe convection. The NMMUJ, FV3 and MPAS kinetic energy spectra show a shallower slope at finer scales, consistent with observations and turbulence theory. FV3 and MPAS produced relatively flat vertical velocity spectra, with a peak at 4-8 times the grid scale, consistent with the effects of poorly resolved convective processes near the grid scale. FV3 vertical motions and orography were somewhat smoother than MPAS. NMMUJ produced much less vertical velocity variability at all scales, and did not show a peak at small scales, despite the fact that it used the highest resolution orography. The reason for this is not clear, although it may be related to the use of divergence damping in the dynamical core and/or the influence of convective parameterization. FV3, MPAS and NIM conserved dry mass well during the forecasts, while NMMUJ lost dry mass. After an initial spinup period the global mean precipitation converged to similar levels in FV3, MPAS and NIM, while the precipitation continued to increase in NMMUJ. The total integrated water vapor in the atmosphere increased steadily in the FV3 and NMMUJ integrations. NIM had larger hourly surface pressure tendency variance compared to the other models, indicating a higher level of spurious external mode gravity wave noise.

FV3 and MPAS both produced similar fine-scale detail in both the vorticity and vertical velocity fields within tropical cyclones. Within tropical cyclones, NMMUJ produced some unrealistic grid-scale noise, and the vertical velocity field did not appear to represent details of the convection embedded in the eyewall and outer rainbands. The NIM forecast tropical cyclones were excessively smooth, lacking any fine-scale detail. The NIM forecasts also did not represent the detailed aspects of the severe convection over the southern Great Plains on 18-20 May, 2013. The other three models all represented some realistic details in the convective outbreak, including the development of cold pools and outflow boundaries. NMMUJ showed a curious tendency to produce vertical motion structures that are anti-correlated at 850 hPa and 500 hPa.

These tests have revealed significant issues with NIM and NMMUJ that may be related to some combination of configuration, numerics and/or physics coupling. These issues should be examined more deeply before any further testing is done with these models.

Acknowledgements:

Jin Lee and Man Zhang of ESRL provided the NIM forecasts. Ratko Vasic and Tom Black of EMC provided provided the NMMUJ forecasts. Bill Skamarock, Joe Klemp and Sang-Hun Park of NCAR provided the MPAS forecasts. Shian-Jiann Lin and Jan-Huey Chen of GFDL provided the FV3 forecasts. All of the aforementioned people collaborated in the design and execution of the tests through discussions on bi-weekly conference calls. Tom Hamill and John Michalakes provided valuable comments on a draft version of this report. Thanks to Tim Schneider and Bonny Strong for their program management efforts, and to the NOAA HPC staff for facilitating the use of the Theia system for running the FV3, NMMUJ and NIM forecasts. Thanks also to NSF and NCAR for providing resources on the Yellowstone supercomputer to produce the MPAS forecasts.

References

Chen, J.-H., and S. J. Lin, 2013: Seasonal Predictions of Tropical Cyclones Using a 25-km-Resolution General Circulation Model. *J. Climate*, **26**, 380–398. doi: http://dx.doi.org/10.1175/JCLI-D-12-00061.1

Donner L. J, and coauthors, 2011: The Dynamical Core, Physical Parameterizations, and Basic Simulation Characteristics of the Atmospheric Component AM3 of the GFDL Global Coupled Model CM3. *J. Climate*, **24**, 3484–3519. doi: http://dx.doi.org/10.1175/2011JCLI3955.1

Ecklund, W. L., K. Gage, G. D. Nastrom, and B. B. Balsley, 1986: A preliminary climatologyo f the spectrum of vertical velocity observed by clear-air Doppler radar, *J. Clim. Appl. Meteorol.*, **25**, 885-892.

Giraldo, F., Kelly, J. , and E. Constantinescu, E. M., 2013: Implicit-explicit formulations of a three-dimensional non-hydrostatic unified model of the atmosphere (NUMA). *SIAM Journal on Scientific Computing*, **35(5)**, B1162-B1194.

Janjic, Z., and R.L. Gall, 2012: Scientific documentation of the NCEP non-hydrostatic multistage model on the B grid (NMMB). Part 1 Dynamics. NCAR Technical Note NCAR/TN-489+STR, doi: 10.5065/D6WH2MZX.

Lin, S.-J., 2004: A vertically Lagrangian Finite-Volume Dynamical Core for Global Models. *Mon. Wea. Rev*., **132**, 2293-2307.

Skaramarock, W, M. Duda, L. Fowler, S.-.H Park and T. Ringler, 2012: A Multi-scale Nonhydrostatic Atmospheric Model Using Centroidal Voronoi Tesselations and C-Grid Staggering. *Mon. Wea. Rev.*, **240**, 3090-3105, doi:10.1175/MWR-D-11-00215.1

Skamarock W., S.-H. Park, J. Klemp, and C. Snyder, 2014: Atmospheric Kinetic Energy Spectra from Global High-Resolution Non-hydrostatic Simulations. *J. Atmos. Sci.*, **71**, 4369–4381. doi: http://dx.doi.org/10.1175/JAS-D-14-0114.1

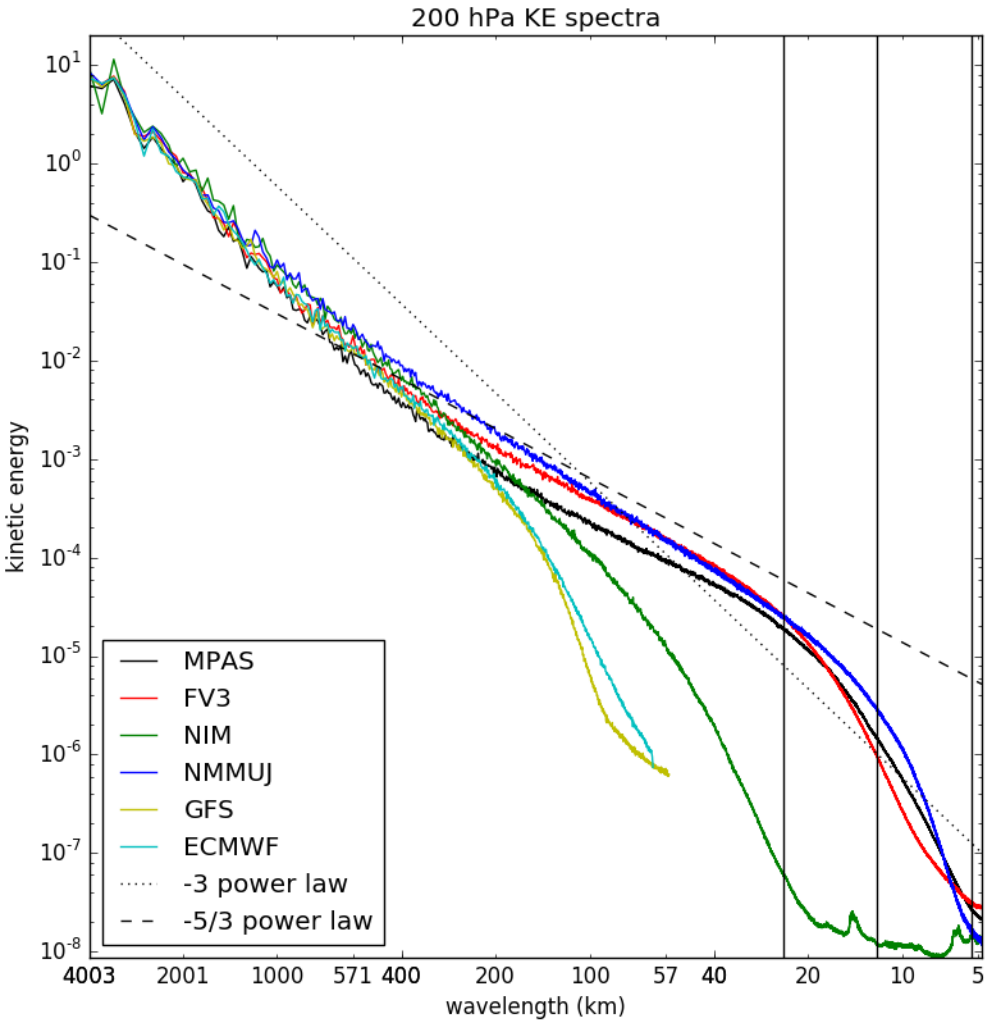

Figure 1 : 200 hPa global kinetic energy spectra (m^2/s^2) for forecast hour 72 of the Hurricane Sandy case. The x-axis is wavelength in km, with values ranging from total wavenumber 10 (~ 4000 km) to wavenumber 7200 (~ 3 km), with a log-scale in total wavenumber. Two reference lines are plotted, one with a slope corresponding to a -3 power-law spectrum (solid black), and one with a slope corresponding to a -5/3 power-law spectrum. The three vertical lines represent wavelengths corresponding to two, four

and eight times the nominal grid resolution (6 km, 12 km and 24 km). The spectra for a T1534 72-hour GFS forecast and operational ECMWF forecast valid at the same time are also shown for reference (the yellow and cyan lines). The GFS spectra were computed from 0.25 degree data, the ECMWF spectra from 0.28125 degree data.

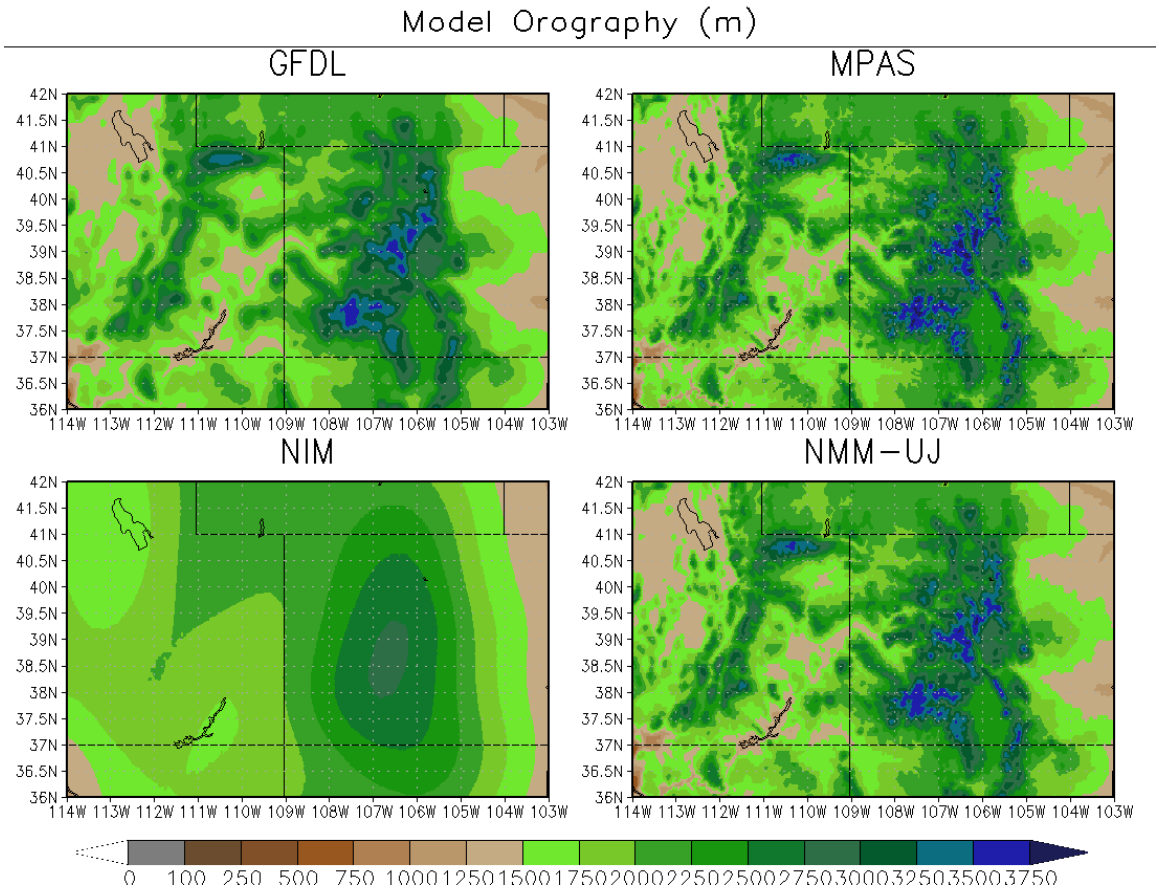

Figure 2: Model orography over the Rocky Mountain region.

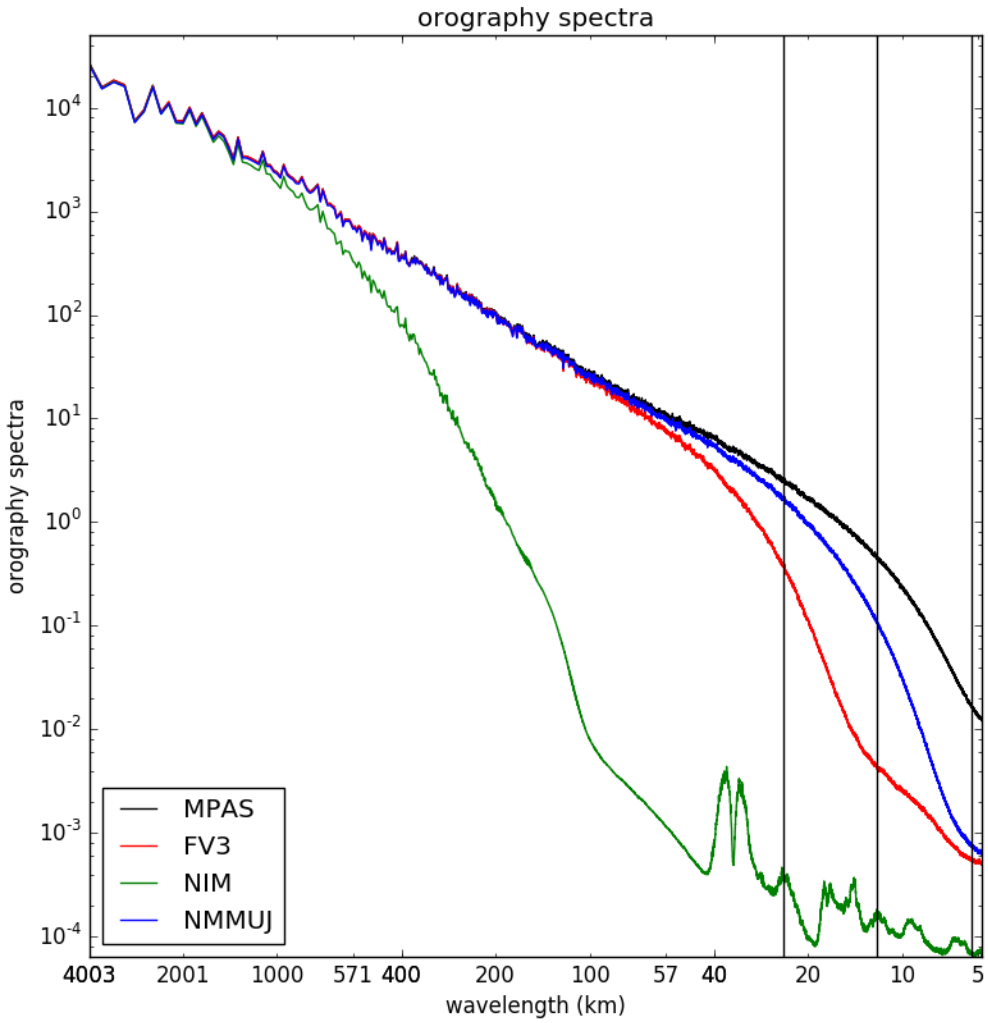

Figure 3: Orography variance spectra (m^2). The x-axis is wavelength in km, with values ranging from total wavenumber 10 (~ 4000 km) to wavenumber 7200 (~ 3 km), with a log-scale in total wavenumber. The three vertical lines represent wavelengths corresponding to two, four and eight times the nominal grid resolution (6 km, 12 km and 24 km)

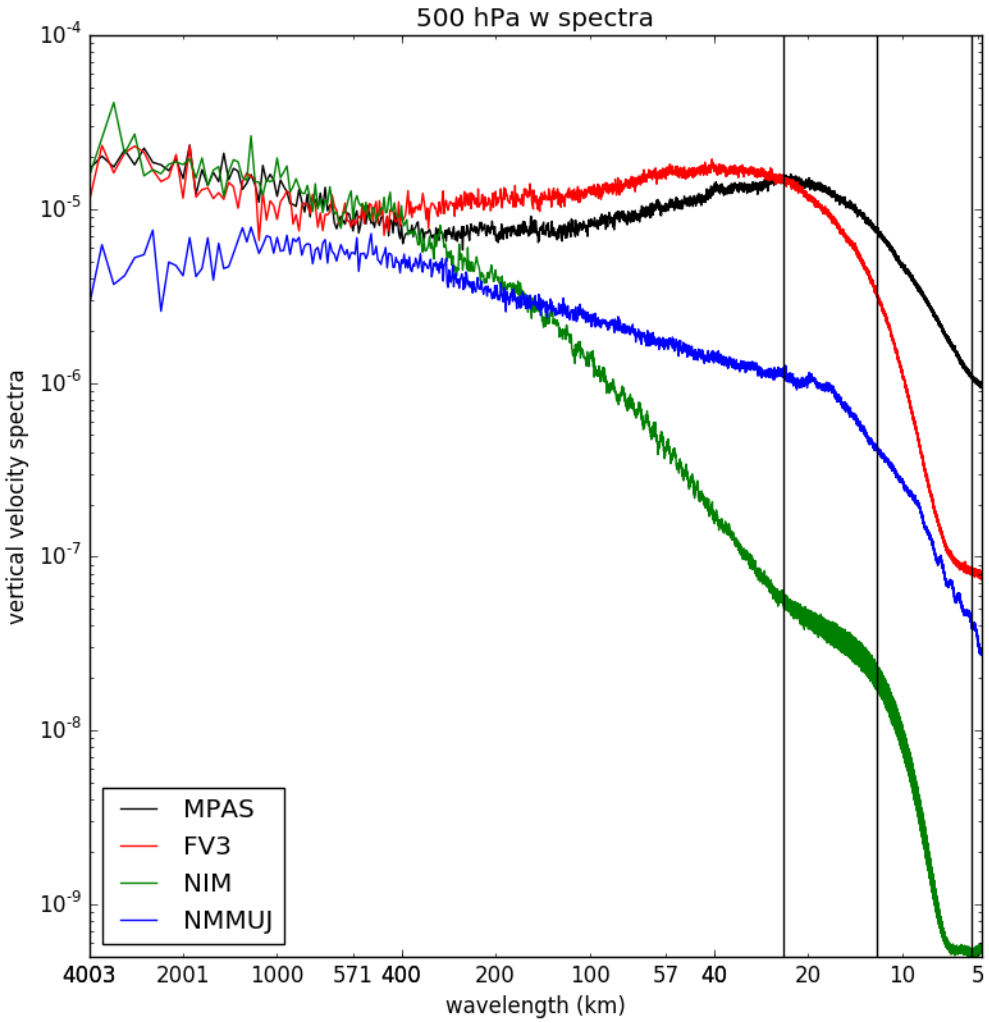

Figure 4: 500 hPa global vertical velocity variance spectra (m^2/s^2) for forecast hour 72 of the Moore tornado case. The x-axis is wavelength in km, with values ranging from total wavenumber 10 (~ 4000 km) to wavenumber 7200 (~ 3 km), with a log-scale in total wavenumber. The three vertical lines represent wavelengths corresponding to two, four and eight times the nominal grid resolution (6 km, 12 km and 24 km).

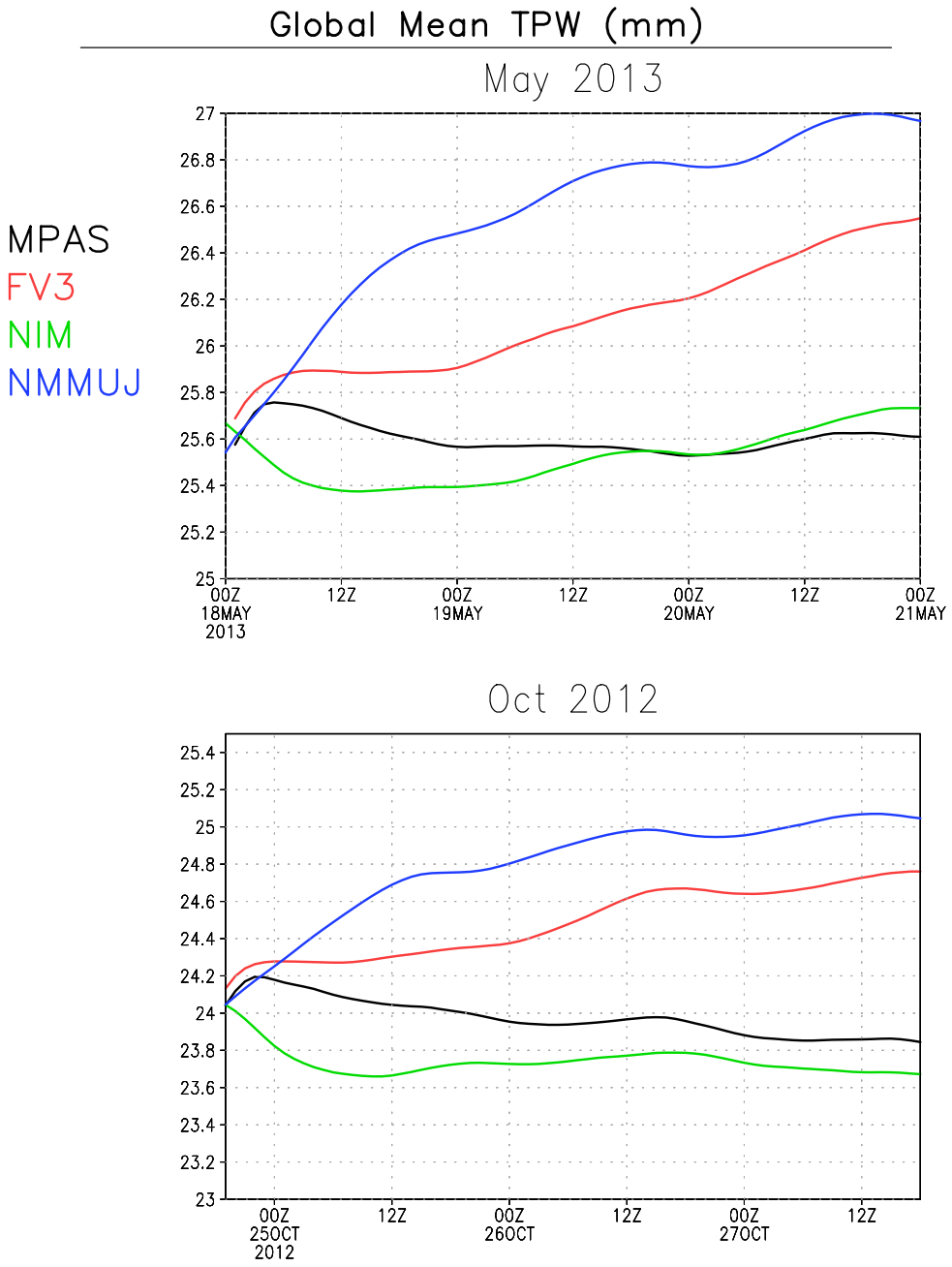

Figure 5: Global mean integrated water vapor (precipitable water) in mm as a function of forecast lead time. Both the Hurricane Sandy and Moore tornado cases are shown.

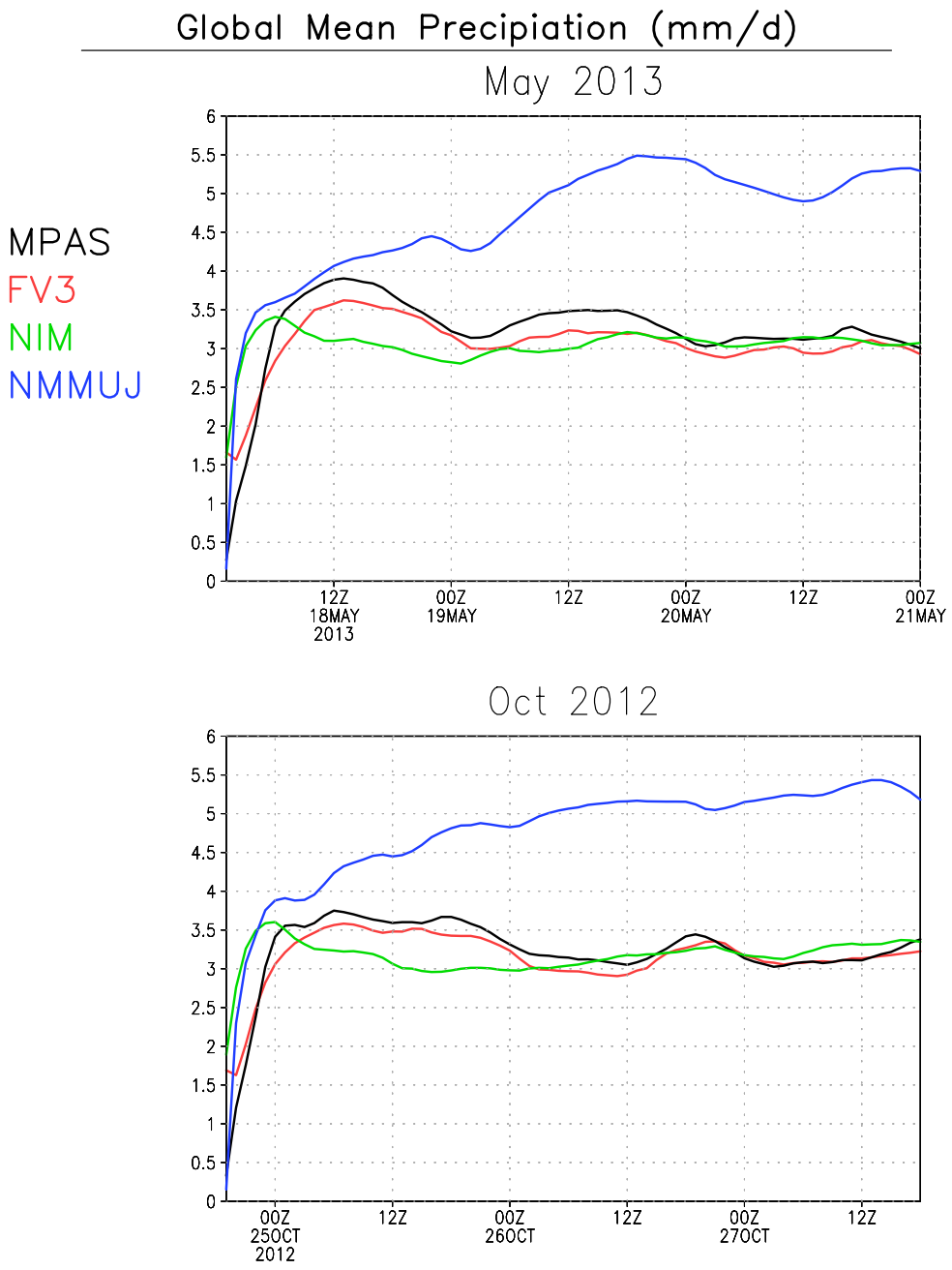

Figure 6: Global mean precipitation (mm per day). Both the Hurricane Sandy and Moore tornado cases are shown.

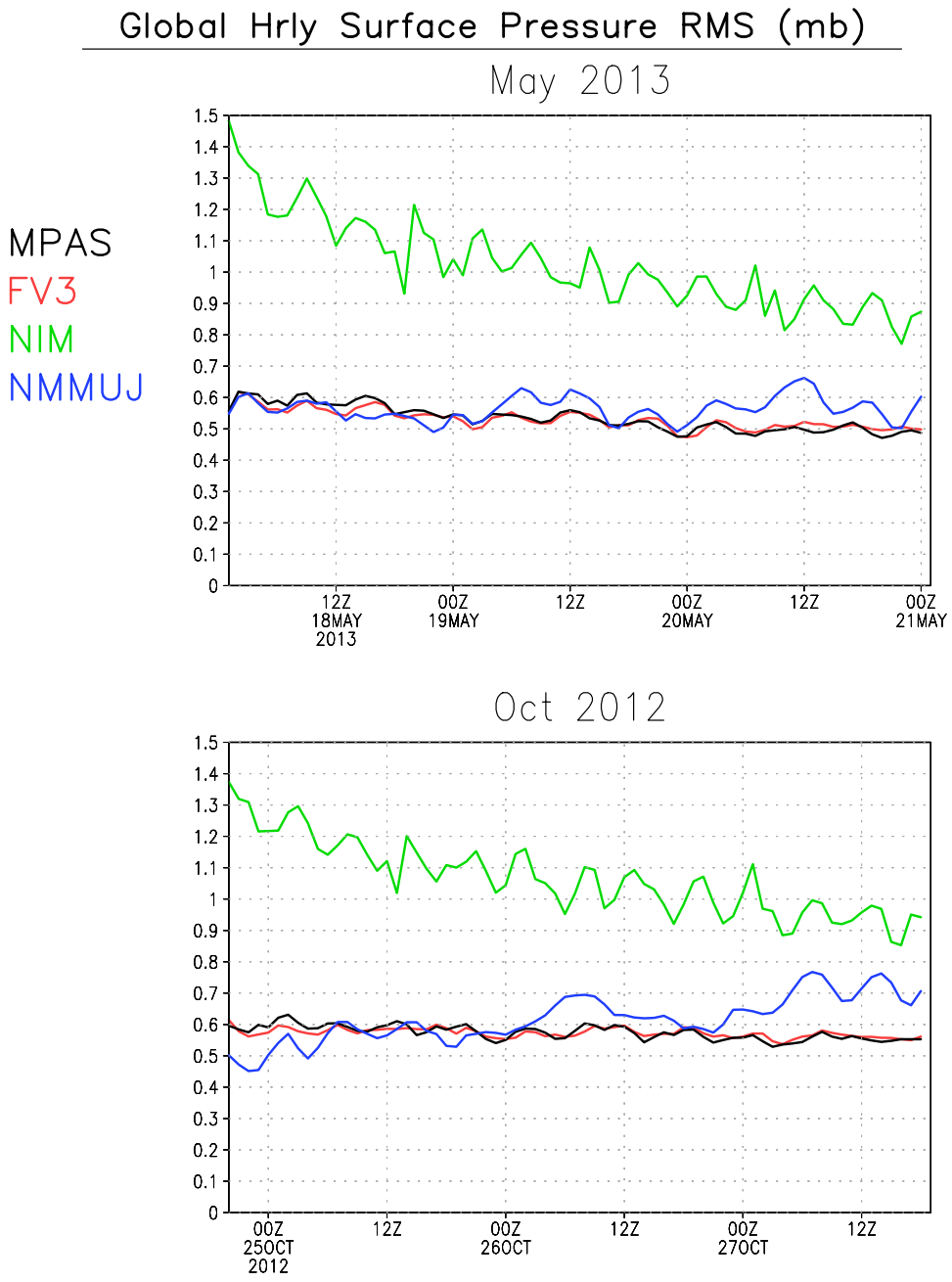

Figure 7: Global mean hourly surface pressure tendency standard deviation (in hPa).

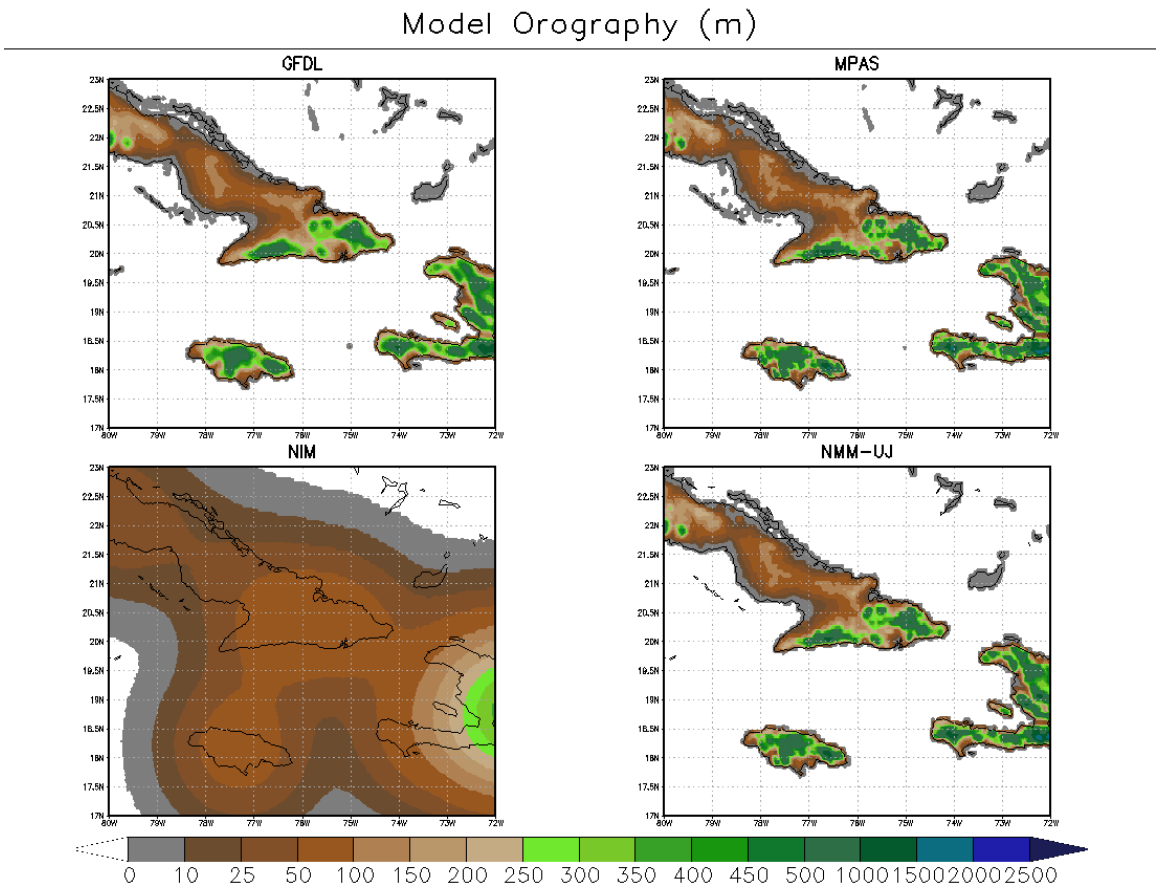

Figure 8: Model orography over Cuba, Jamaica and western Hispaniola.

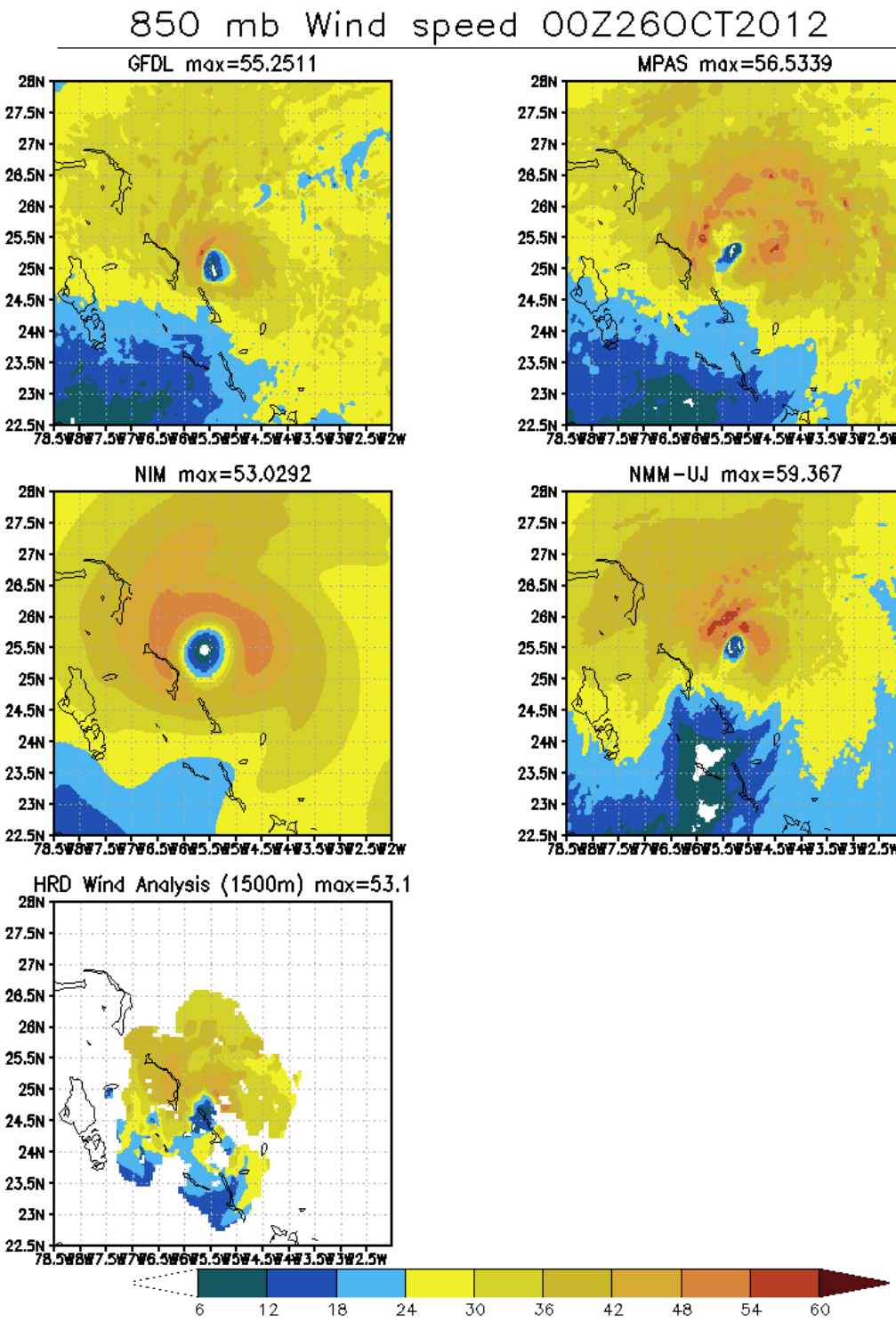

Figure 9: 30-h forecast 850 hPa wind speed (in meters per second) and the HRD radar estimated wind speed at 1500-m for 00UTC 26 October 2012.

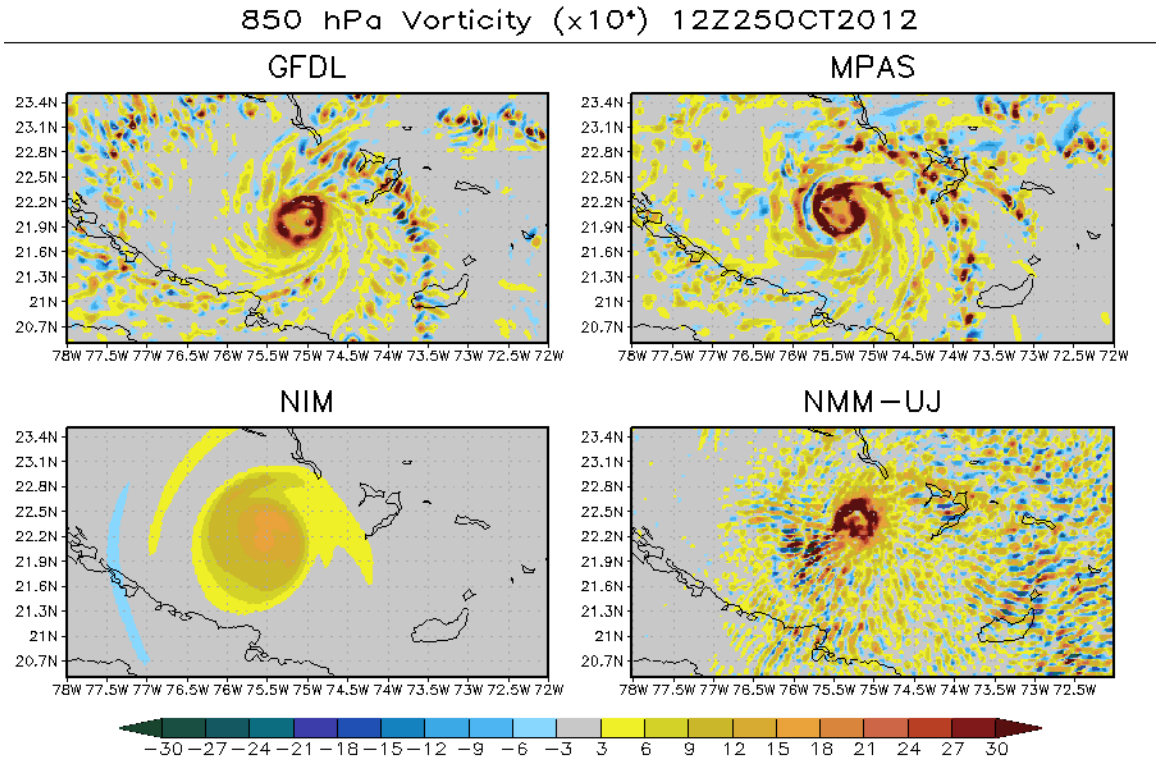

Figure 10: 18-h forecast 850hPa relative vorticity for Hurricane Sandy valid 12UTC October 25, 2012.

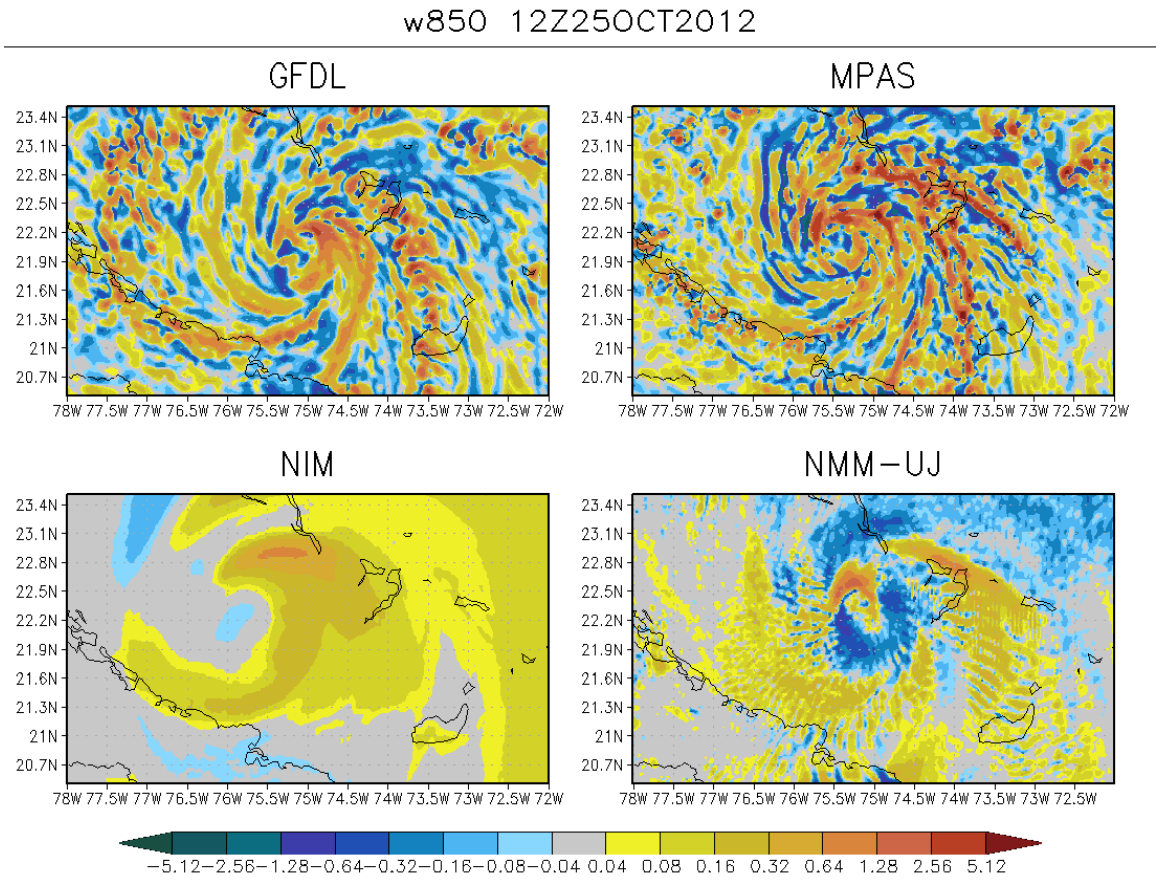

Figure 11: 18-h forecast 850hPa vertical velocity (ms^{-1}) for Hurricane Sandy valid 12UTC October 25, 2012.

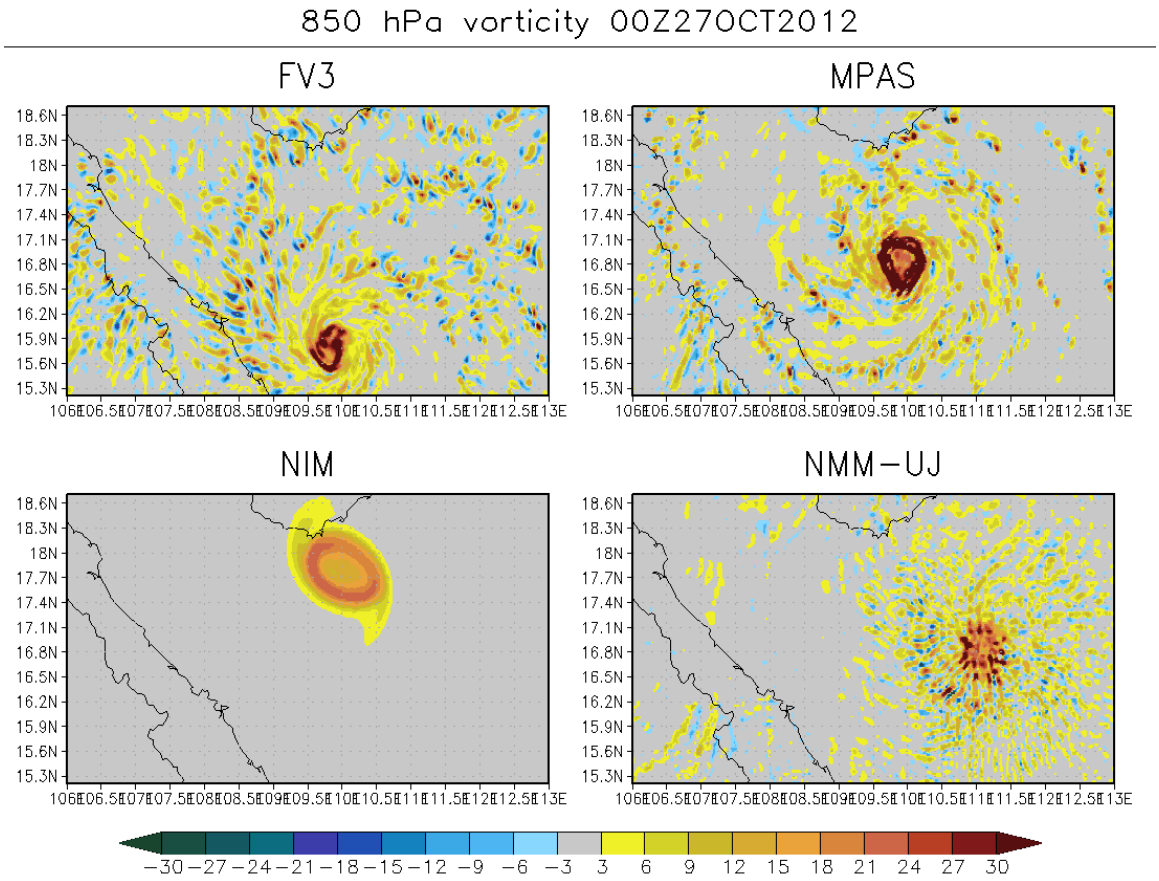

Figure 12: 54-h forecast 850hPa relative vorticity for Typhoon Son-Tinh valid 00UTC October 27, 2012.

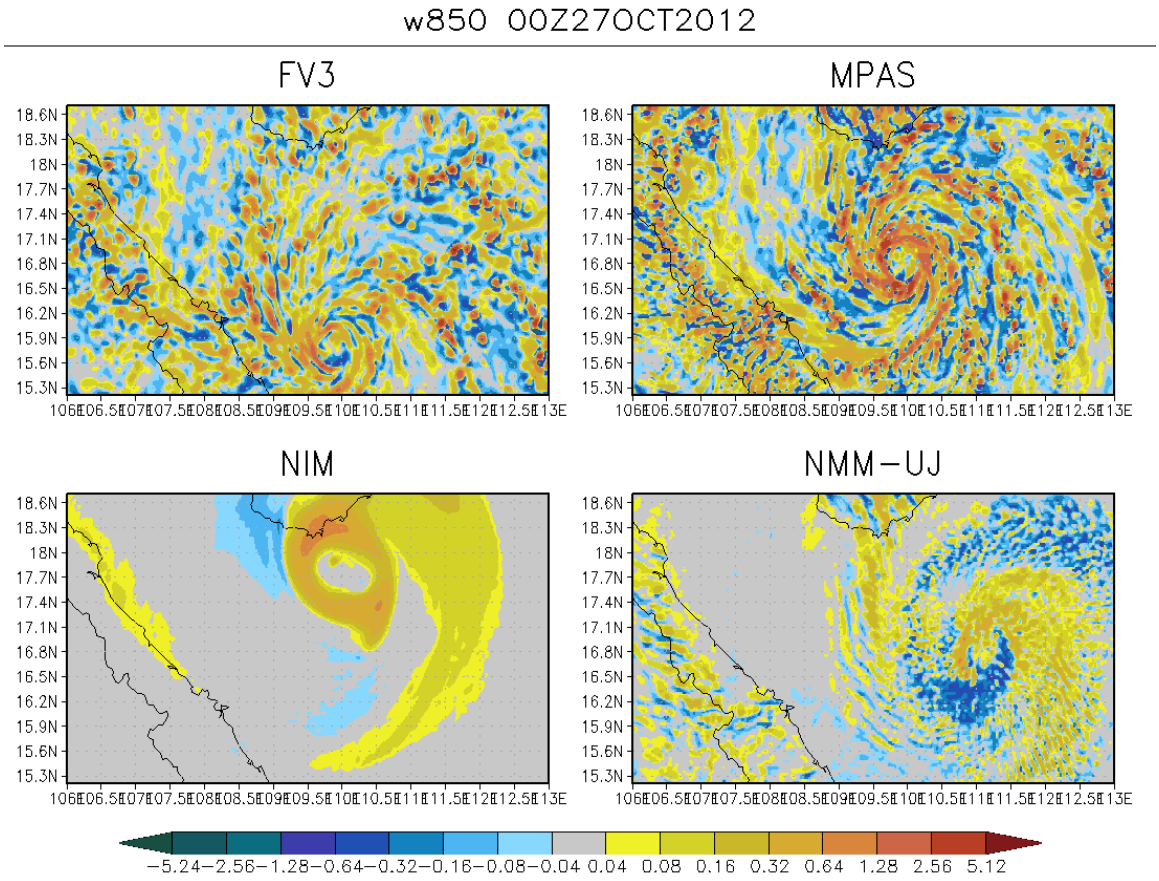

Figure 13: 54-h forecast 850hPa vertical velocity for Typhoon Son-Tinh valid 00UTC October 27, 2012.

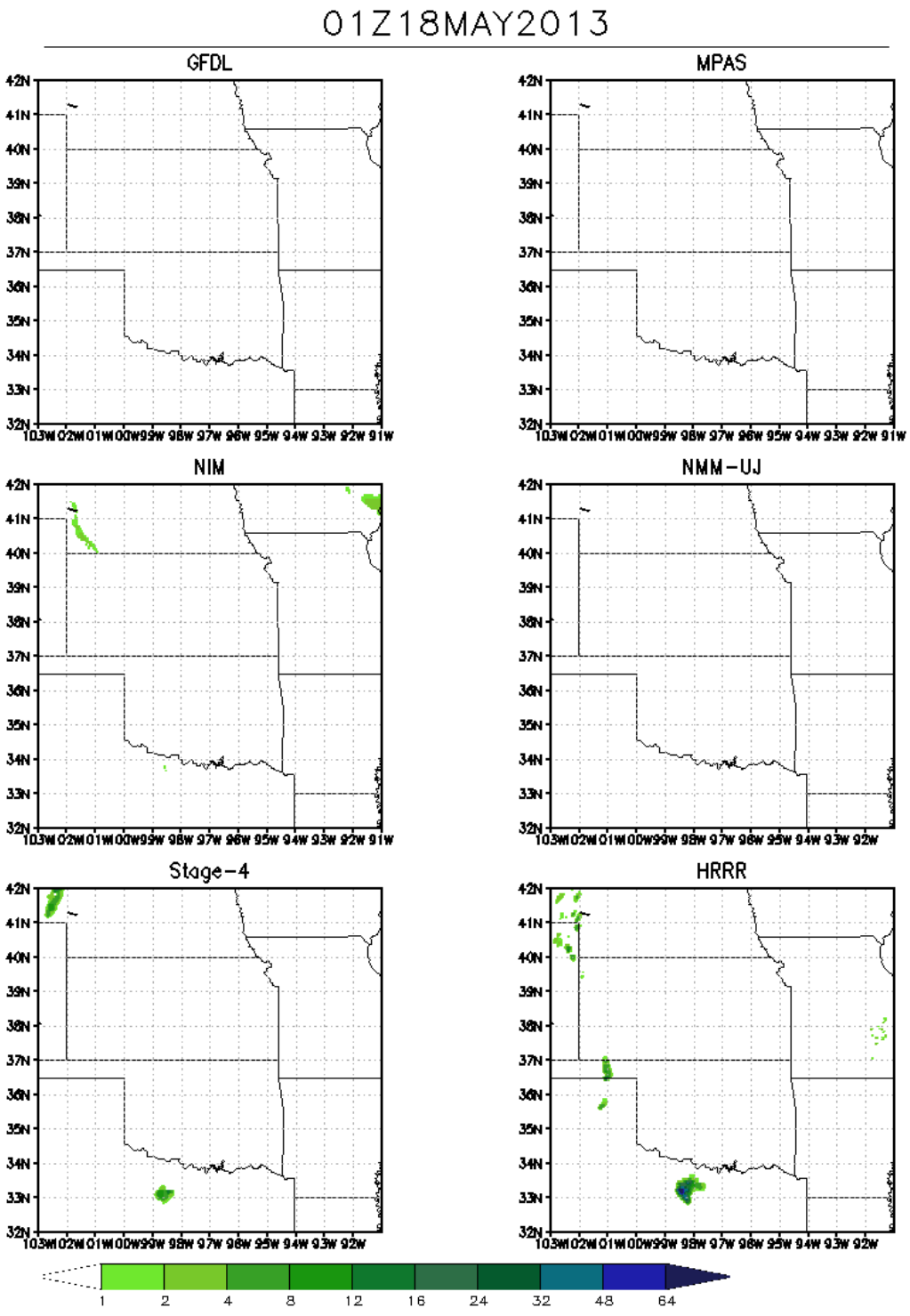

Figure 15: Animation of 1-hour accumulated precipitation (mm) over the south-central Great Plains for May 18-20, 2013 for the four model forecasts, plus Stage IV estimated precipitation and 1-h accumulated precipitation from HRRR forecasts. The figure image is a hyperlink to an animation at http://www.esrl.noaa.gov/psd/forecasts/hiwpp/precip.html.

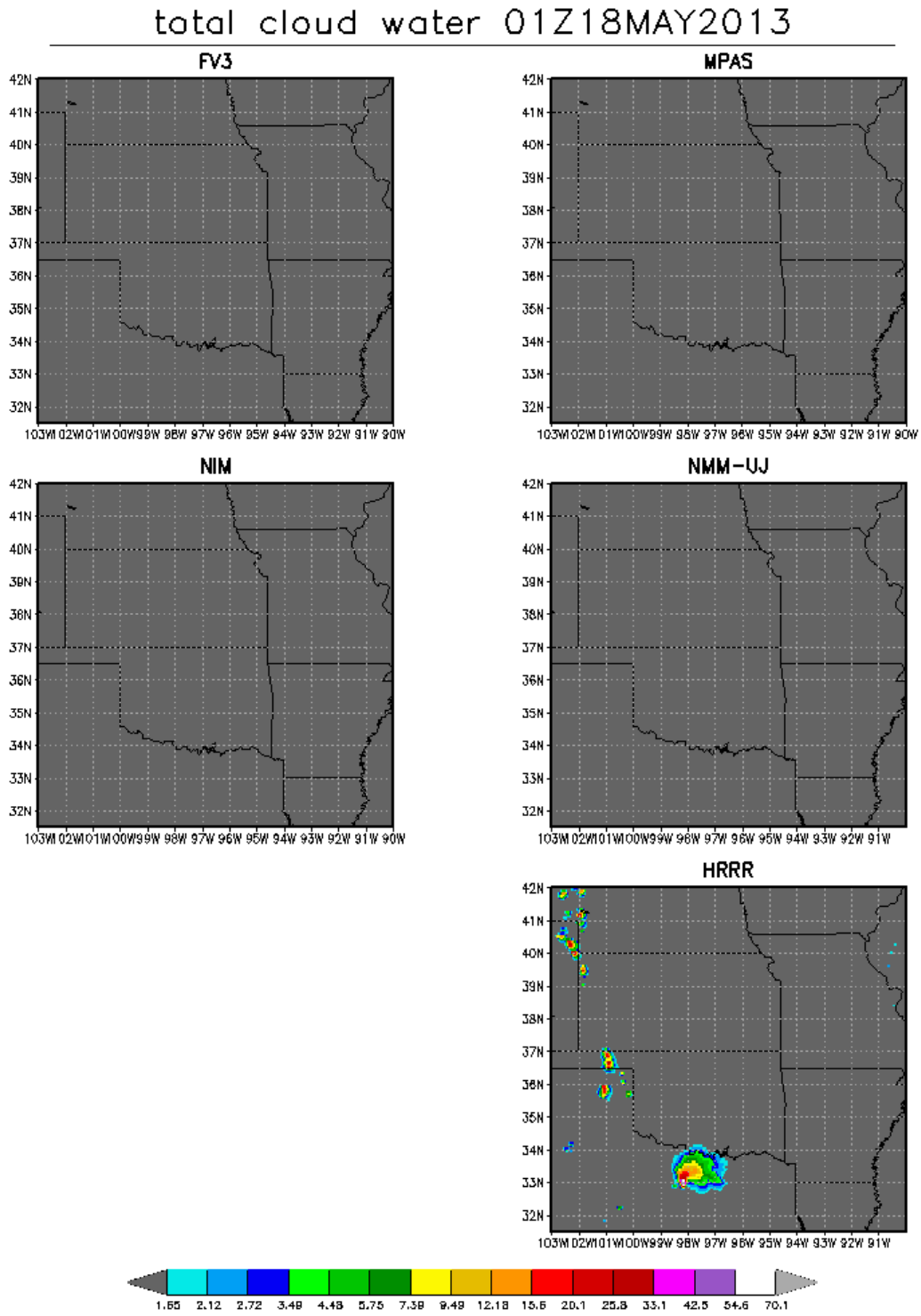

Figure 15: Animation of total cloud condensate (in mm) over the south-central Great Plains for May 18-20, 2013 for the four model forecasts, and from 1-h accumulated HRRR forecasts valid at the same time. The figure image is a hyperlink to an animation at http://www.esrl.noaa.gov/psd/forecasts/hiwpp/tcw.html.

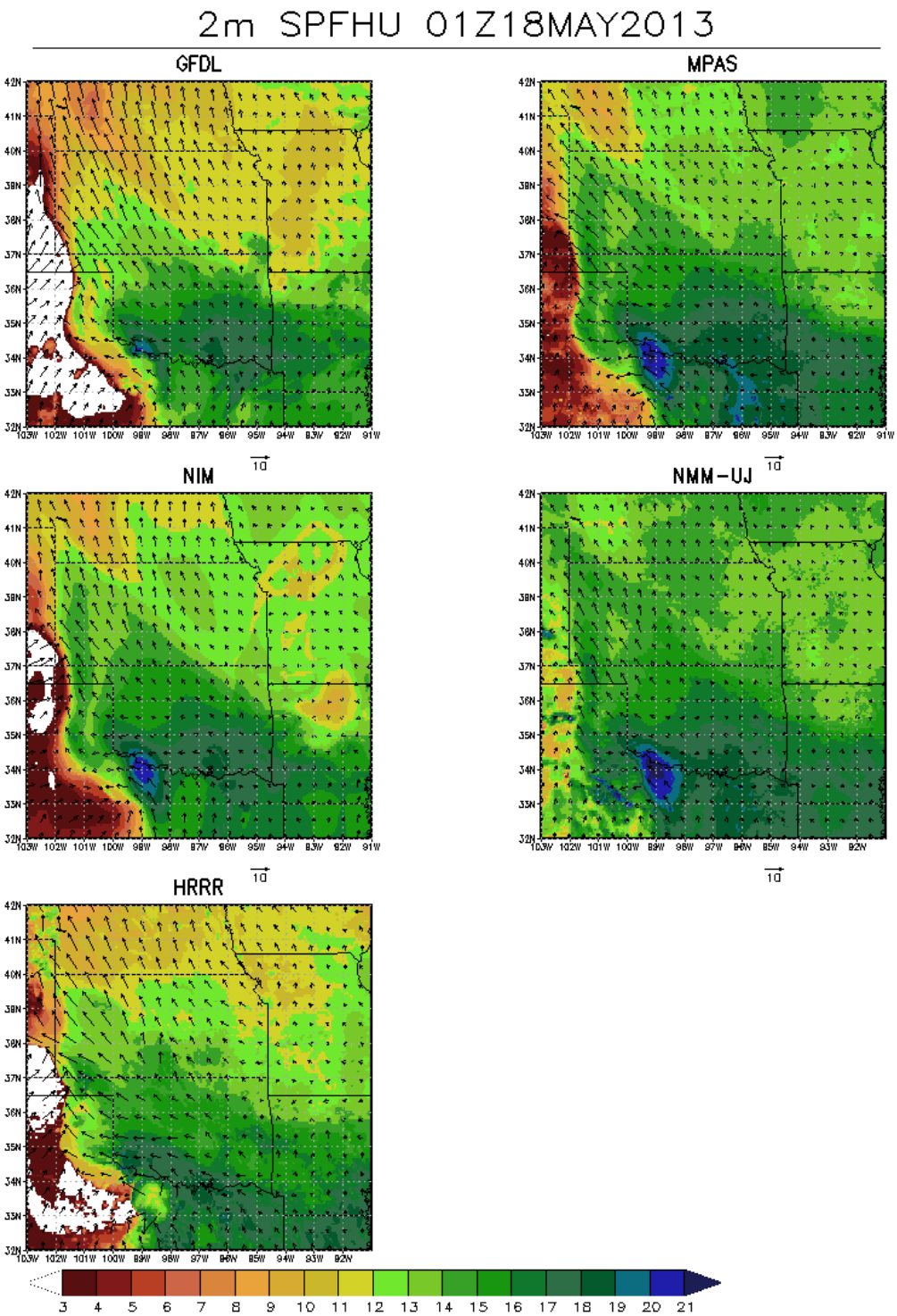

Figure 16: Animation of 2-meter specific humidity (in grams per kg) and 10-m wind vectors over the south-central Great Plains for May 18-20, 2013 for the four model forecasts, and from 1-h HRRR forecasts valid at the same time. The power used in the transform is 0.33. The figure image is a hyperlink to an animation at http://www.esrl.noaa.gov/psd/forecasts/hiwpp/q2m.html.

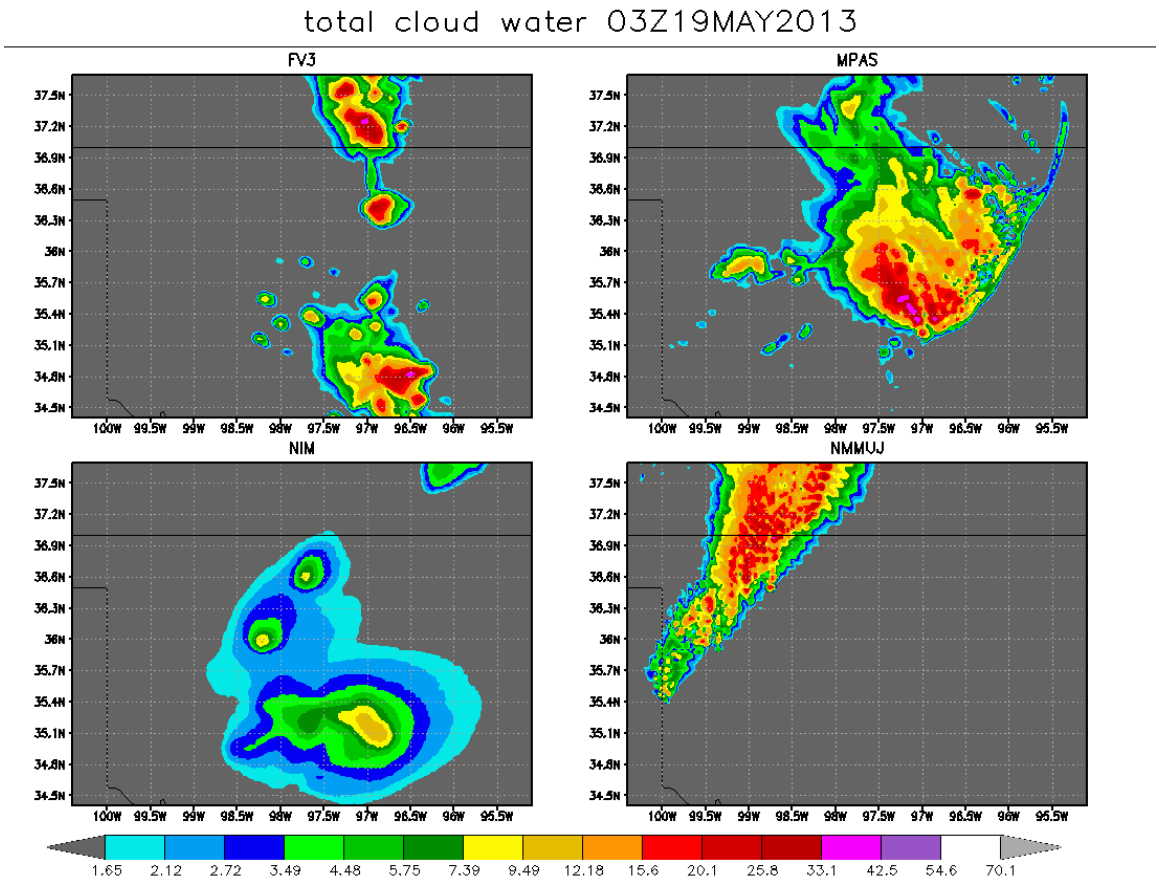

Figure 17: 27-h forecast total cloud condensate in a 3.3 degree by 5.3 degree (lat/lon) box over northwest Oklahoma valid 00UTC 19 May 2013.

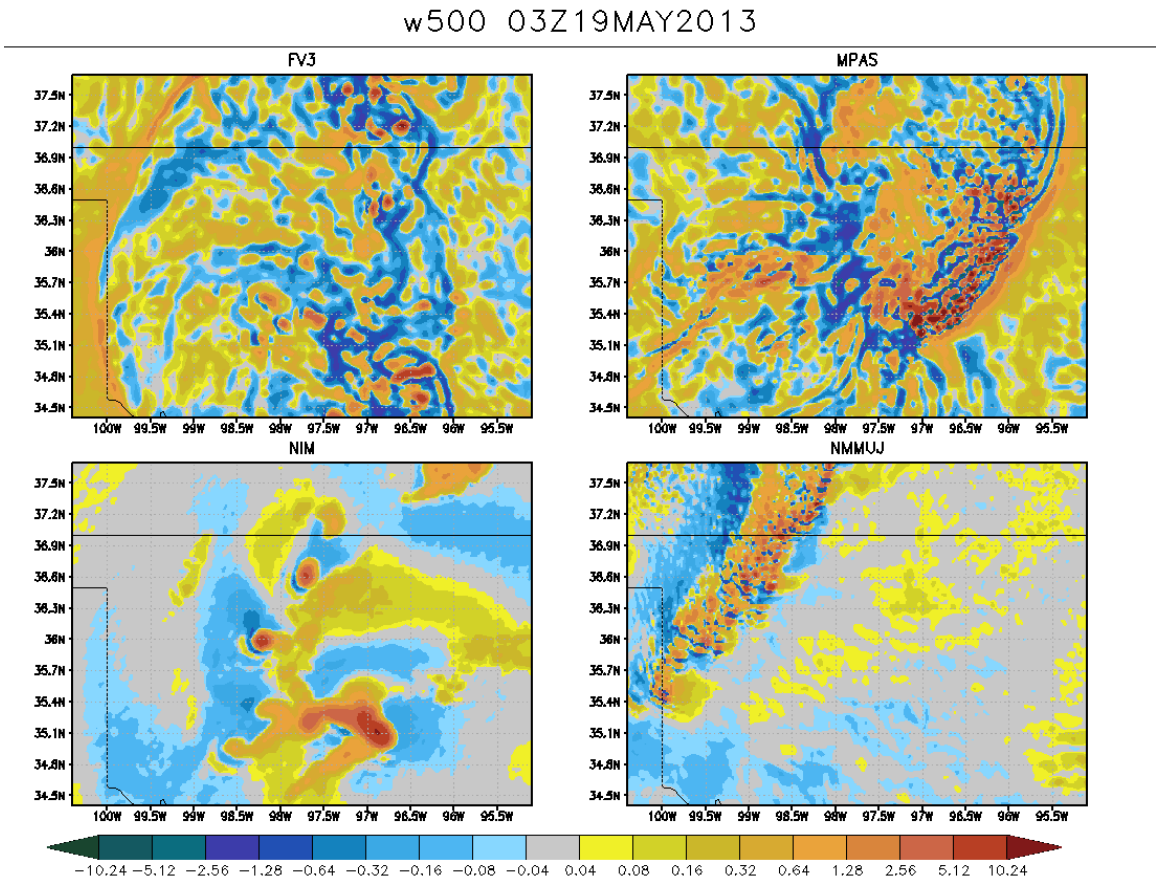

Figure 18: 27-h forecast 500 hPa vertical velocity in a 3.3 degree by 5.3 degree (lat/lon) box over northwest Oklahoma valid 03UTC 19 May 2013.

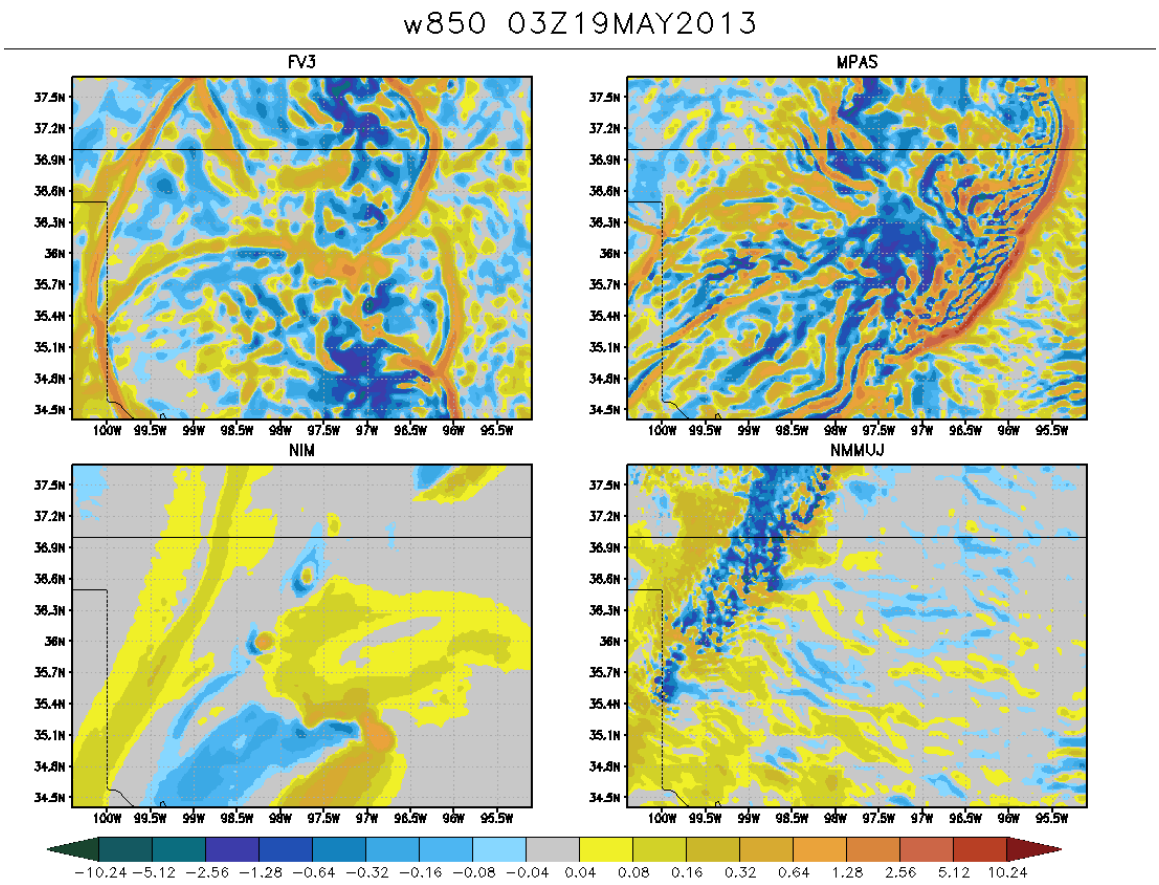

Figure 19: As in Figure 18, but for 850hPa.